(Z)-7,4'-dimethoxy-6-hydroxy-aurone-4-O-β-glucopyranoside attenuates lipoteichoic acid-induced damage in rat cardiomyoblast cells

Qiang Song[1], Xuegang Xie[1], Zhi Hu[1], Jianying Xue[1], Songlin Zhang[1] and Xinming Xie[2] ⓘD

Abstract

Objective: Excessive inflammatory responses in the endocardium are related to progression of infectious endocarditis. This study aimed to investigate whether (Z)-7,4'-dimethoxy-6-hydroxy-aurone-4-O-β-glucopyranoside (DHAG), a compound isolated from the endophytic fungus *Penicillium citrinum* of *Bruguiera gymnorrhiza*, could attenuate cell damage caused by lipoteichoic acid (LTA) in embryonic rat heart cells (H9c2).

Methods: LTA-induced cell damage occurred in H9c2 cells and the protective effects of DHAG at different concentrations (1–10 μM) were assessed. Indicators of oxidative stress and inflammatory responses in H9c2 cells were measured.

Results: DHAG (1–10 μM) significantly attenuated LTA-induced damage in H9c2 cells, as evidenced by increased cell viability and mitochondrial membrane potential, decreased cytochrome c release and DNA fragmentation, inhibition of caspase-3 and -9 activity, and altered expression of apoptosis-related proteins. DHAG also decreased oxidative stress by increasing protein expression of nuclear factor (erythroid-derived 2)-like 2 (Nrf2). Furthermore, DHAG inhibited inflammatory responses by decreasing protein expression of nuclear factor kappa B (NF-κB) and mitogen-activated protein kinases (MAPKs).

[1]Department of Structural Heart Disease, the First Affiliated Hospital of Medical College, Xi'an Jiaotong University, Xi'an, China
[2]Department of Respiratory and Critical Care Medicine, the First Affiliated Hospital of Medical College, Xi'an Jiaotong University, Xi'an, China

Corresponding author:
Xinming Xie, Department of Respiratory and Critical Care Medicine, the First Affiliated Hospital of Xi'an Jiaotong University, No. 277, Yanta West Road, Xi'an 710061-China.
Email: xiexm1527@163.com

Conclusion: DHAG exerted protective effects against LTA-induced cell damage, at least partially by decreasing oxidative stress and inhibiting inflammatory responses. Our results provide a scientific rational for developing DHAG as a therapy against infectious endocarditis.

Introduction

Infective endocarditis (IE) results from infection of the endocardium by bacteria (commonly *Streptococcus sanguinis*) or fungi, and may cause cardiac complications such as fever, petechiae, anemia, and valvular incompetence or obstruction.[1,2] Unfortunately, little is known regarding the molecular mechanisms causing IE.[3,4] Current treatments include intravenous antibiotics, valve debridement, valve repair or replacement and surgery. However, few effective therapies are available for patients with IE.[2,5,6] Therefore, the search for novel therapeutic strategies is critically important.

As the smallest bioactive peptidoglycan fragment present in the membranes of Gram-positive bacteria, lipoteichoic acid (LTA) is a major antigen recognized by innate immune cells such as macrophages and monocytes and is well-known for its induction of inflammatory responses.[7,8] Studies showed that LTA triggered activation of cardiomyocytes and induced a diverse array of inflammatory responses by promoting the release of various pro-inflammatory cytokines and mediators, including nitric oxide (NO), interleukin (IL)-1β, IL-6, and tumor necrosis factor alpha (TNF-α) through the phosphorylation of nuclear factor-κB (NF-κB).[9] Over-production of pro-inflammatory factors resulted in toxic intracellular events, resulting in cell death.[10] Excessive amount of pro-inflammatory cytokines can be detected in IE and these cytokines stimulate oxidant production in the myocardium with subsequent peroxidative damage to macromolecules. Oxidative stress has been shown to play a crucial role in the IE progression.[11]

Herbal plants are an important source of medicinal products. Supplementation of exogenous antioxidants might alleviate oxidative damage and different antioxidants have been used to effectively treat disorders caused by oxidative stress.[12–14] (Z)-7,4'-dimethoxy-6-hydroxy-aurone-4-O-β-glucopyranoside (DHAG), a compound isolated from the endophytic fungus *Penicillium citrinum* of *Bruguiera gymnorrhiza.*, was shown to have neuroprotective effects via inhibition of oxidative stress.[15] Furthermore, DHAG was also found to inhibit LTA-induced production of inflammatory factors in our preliminary study. In the present study, the protective effects of DHAG against LTA-induced inflammatory responses and oxidative stress in cardiomyoblasts were investigated.

Materials and methods

Cell lines, reagents and chemicals

The cardiomyoblast cell line H9c2 was purchased from Beijing Cell bank

(Beijing, China). Fetal bovine serum and RPMI-1640 medium were from Gibco BRL (Gaithersburg, MD, USA). LTA and 3-(4,5-dimethylthiazol)-2,5-diphenyltetrazolium-bromide (MTT) were purchased from Sigma-Aldrich (St. Louis, MO, USA). Caspase-3/9 activity assay kits were from Promega (Madison, WI, USA). Glutathione (GSH), superoxide dismutase (SOD), malondialdehyde (MDA), IL-1β, and TNF-α assay kits were purchased from Jiancheng Biological Engineering (Nanjing, China). The cytochrome c assay kit was from R&D systems (Minneapolis, MN, USA). 5,5′,6,6′-tetrachloro-1,1′,3,3′-tetraethylbenzimidazolylcarbocyanine iodide (JC-1) and 2′,7′-dichlorofluorescin diacetate (DCFH-DA) were purchased from Molecular Probes (Eugene, OR, USA). Real-time PCR reagents were purchased from Thermo Fisher (Waltham, MA, USA). DHAG was provided by Prof. Teng from Zhengzhou University.[15] All solvents and chemicals were analytical grade and were purchased from Sinopharm Chemical Reagent Co. Ltd. (Shanghai, China). LTA and DHAG were dissolved in dimethyl sulfoxide (DMSO).

Cell culture and treatment

H9c2 cells were cultured in RPMI-1640 medium supplemented with 10% fetal bovine serum and 1% streptomycin/penicillin at 37°C under a humidified atmosphere containing 5% CO_2. H9c2 cells were treated with DHAG at 1, 3, or 10 μM for 6 hours, then with LTA at 10 μg/mL for 24 hours. Cells were treated with DMSO as a negative control.

Cell viability assay

Cytotoxicity was assessed using an MTT-based colorimetric assay. After treatment, MTT solution was added to each well to a final concentration of 62.5 μg/mL and mixed well. After incubation for 4 hours at 37°C, the supernatant was removed and the formazan produced in viable cells was solubilized with 200 μL of DMSO. The absorbance in each well was measured at 570 nm using an enzyme-linked immunosorbent assay (ELISA) microplate reader.

Mitochondrial membrane potential (MMP) measurement

MMP was measured using the fluorescent probe JC-1. After treatment, H9c2 cells were incubated with 2 μM JC-1 at 37°C for 15 min in the dark. After washing, fluorescence was measured using a fluorescence reader with excitation at 490 nm and emission at 590/530 nm.

Cytochrome c measurement

H9c2 cells were fractionated after treatment. Levels of cytochrome c were measured using an assay kit according to the manufacturer's instructions. Optical density was measured at 490 nm using an ELISA plate reader.

DNA fragmentation measurement

After treatment, H9c2 cells were lysed and DNA fragmentation was measured using a Cell Death Detection ELISAplus kit according to the manufacturer's instructions. The optical density was measured at 405 nm using a microplate reader.

Caspase activity measurement

Caspase-3/9 activities were measured according to the manufacture's protocol. Briefly, 100 μL of reagent for specific caspase were added into each well and the plate was then incubated at room temperature for 3 hours. Luminescence was measured using a microplate reader.

SOD activity, MDA and GSH level

SOD activity and MDA and GSH levels were measured using assay kits according to the manufacturer's protocols. Briefly, after washing, H9c2 cells were homogenized and the supernatant was used to measure SOD, MDA and GSH.

Measurement of reactive oxygen species (ROS)

Intracellular ROS were measured using the fluoroprobe DCFH-DA. H9c2 cells were incubated with DCFH-DA for 30 min in the dark. After washing twice, fluorescence intensity was measured at 488/525 nm using a fluorescence microplate reader.

Cytokine measurement

After treatment, supernatants of culture medium were collected. Levels of IL-1β and TNF-α were quantified using enzyme-linked immunosorbent assay (ELISA) kits according to the manufacturer's instructions.

NO measurement

NO was measured using a Griess assay (Sigma-Aldrich).[16]

Real-time RT-PCR

Total RNA was extracted from H9c2 cells using 1 mL of TRIzol reagent. RNA (0.5 μg) was reverse transcribed into cDNA using a PrimeScript^{TM} RT reagent kit (Takara, Japan). Real-time RT-PCR was performed on a StepOne system (Thermo Fisher) using SYBR green Supermix (Thermo Fisher) and the comparative C_t value method. Expression data were normalized to the geometric mean of the β-actin housekeeping gene. The gene-specific primer sequences used were as follows: iNOS, forward: agggagtgttgttccaggtg, reverse: tcctcaacctgctcctcact, NCBI reference: NM_012611.3; IL-1β, forward:
agtctgcacagttccccaac, reverse: agacctgacttggcagagga, NCBI reference: NM_031512.2; TNFα, forward: gaaacacacgagacgctgaa, reverse: cagtctgggaagctctgagg, NCBI reference: NM_012675.3.; and β-actin, forward: gtcgtac cactggcattgtg, reverse: tctcagctgtg gtggtgaag, NCBI reference: NM_031144.3.

Western blotting

H9c2 cells were harvested in protein lysis buffer containing protease inhibitors and phosphatase inhibitors. Total protein content was determined using Bradford reagent (Beyotime, Shanghai, China). Equal amounts of protein (45 μg) were mixed with 4× loading buffer and separated in 12% (w/v) SDS-polyacrylamide gels. Proteins were then transferred onto polyvinylidene fluoride membranes. Membranes were blocked in Tris-buffered saline containing 1% bovine serum albumin and 0.1% Tween-20 for 1 hour at room temperature. The membranes were incubated with primary antibodies [anti-cleaved caspase-3 rabbit polyclonal (p)Ab ab49822, 1:1000; anti-cleaved caspase-9 (Asp353) rabbit pAb #9507, 1:1000; anti-Bcl-2 rabbit pAb ab196495, 1:1000; anti-Bax rabbit monoclonal (m)Ab ab32503, 1:1000; anti-NADPH oxidase 4 rabbit pAb ab154244, 1:1000; anti-HO-1 rabbit pAb ab13243, 1:1000; anti-Nrf2 rabbit pAb ab137550, 1:1500; anti-P65 rabbit pAb ab16502, 1:1000; anti-P65 (phosphor-S536) rabbit pAb ab86299, 1:1000; anti-P38 rabbit mAb, ab170099, 1:1000; anti-P38 (phosphor-Y182) rabbit pAb, ab47363, 1:1000; anti-JNK rabbit mAb, ab179461, 1:1000; anti-JNK (phospho-T183+T183+T221) rabbit mAb, ab124956, 1:1000; and anti-β-actin, rabbit pAb, ab16039,1:3000] at 4°C overnight. After washing, membranes were incubated with horseradish peroxidase (HRP)-conjugated secondary antibody (goat anti-rabbit IgG H&L HRP, ab6721, 1:3000) for 1 hour at room temperature. All antibodies were from Abcam (Cambridge

UK) except for anti-cleaved caspase-9 (Asp353) rabbit pAb, which was purchased from Cell Signaling Technology (Danvers, MA, USA). Antibody binding was visualized using an enhanced chemiluminescence system (Millipore, Billerica, MA, USA).

Statistical analysis

Data were expressed as mean ± standard deviations and analyzed with SPSS 19.0 software (SPSS Inc., Chicago, IL, USA). The Kolmogorov-Smirnov test was used to assess normality. Dunnett's t test was used to compare the experimental group with the control group. Differences between two groups were compared using the t-test. Differences among multiple groups were compared using one-way analysis of variance. Values of $p < 0.05$ were considered statistically significant. Samples were measured in triplicate and each experiment was repeated three times.

Results

DHAG treatment had no effect on H9c2 cell viability

H9c2 cells were treated with DHAG at 1, 3, or 10 μ M for 48 hours. No obvious changes in cell viability were observed by MTT assay compared with negative control cells, suggesting that DHAG treatment at 10 μM did not damage H9c2 cells (Figure 1).

DHAG treatment attenuated LTA-induced H9c2 cell damage

LTA was toxic to H9c2 cells. However, pre-treatment with DHAG increased cell viability (Figure 2a), increased MMP (Figure 2b), decreased cytochrome c release (Figure 2c), decreased DNA fragmentation (Figure 2d), decreased caspase activities (Figure 2e), and changed the expression levels of apoptosis-related proteins (Figure 2f).
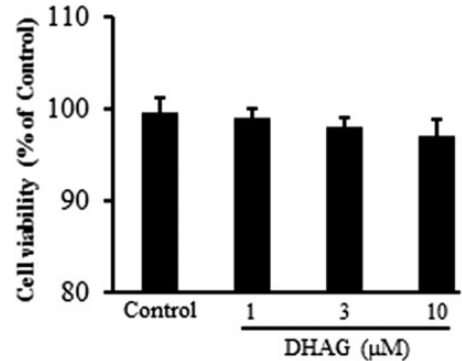

Figure 1. H9c2 cells were treated with DHAG at 1, 3, or 10 μM for 48 hours and cell viability was assessed using an MTT assay. DHAG caused no obvious cytotoxicity in H9c2 cells.

DHAG treatment decreased oxidative stress

Oxidative stress significantly increased following LTA treatment. However, pretreatment with DHAG significantly reduced production of ROS and MDA and increased GSH levels and SOD activities. Moreover, DHAG pre-treatment decreased NADPH oxidase 4 protein expression and increased protein expression of nuclear Nrf2 and HO-1, indicating that DHAG treatment effectively inhibited oxidative stress induced by LTA (Figure 3).

DHAG treatment inhibited inflammatory responses in H9c2 cells

Pro-inflammatory mediators are also inflammatory markers and are present in activated cells. DHAG significant inhibited production of NO, IL-1β and TNF-α in LTA-stimulated H9c2 cells. Levels of *iNOS*, *IL-1β* and *TNF-α* mRNA also increased following exposure to LTA, but decreased following DHAG treatment. Moreover, levels of p-p65, p-JNK and p-p38 proteins increased following LTA stimulation, but decreased following DHAG treatment in a dose-dependent manner (Figure 4).
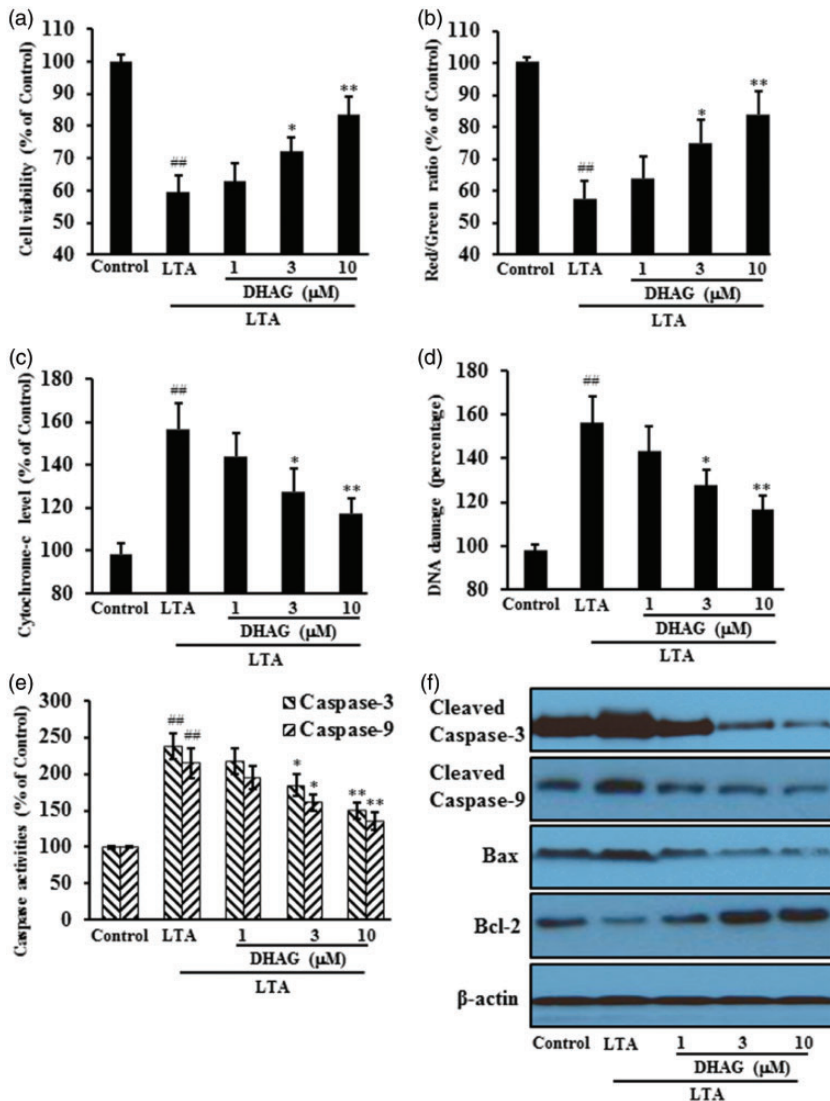
Figure 2. DHAG protected H9c2 cells against LTA-induced cell damage. H9c2 cells were treated with DHAG at 1, 3, or 10 µM for 6 hours then with LTA for 24 hours. Cells were collected to measure cytotoxicity via cell viability (a), mitochondrial membrane potential (b), cytochrome c release (c), DNA damage (d), and caspase activities (e). Expression of apoptosis-related proteins was also assessed by western blotting (f). $^{###}p < 0.01$ vs. negative control; $^{*}p < 0.05$, $^{**}p < 0.01$ vs. LTA alone.

Discussion

The results of our study demonstrated that DHAG, a novel antioxidant, induced expression of Nrf2, which appeared to be involved in intracellular defense against LTA-mediated inflammatory responses. DHAG decreased oxidative stress and production of pro-inflammatory cytokines. Furthermore, DHAG suppressed LTA-mediated activation of upstream signaling molecules, including NF-κB and MAPKs,
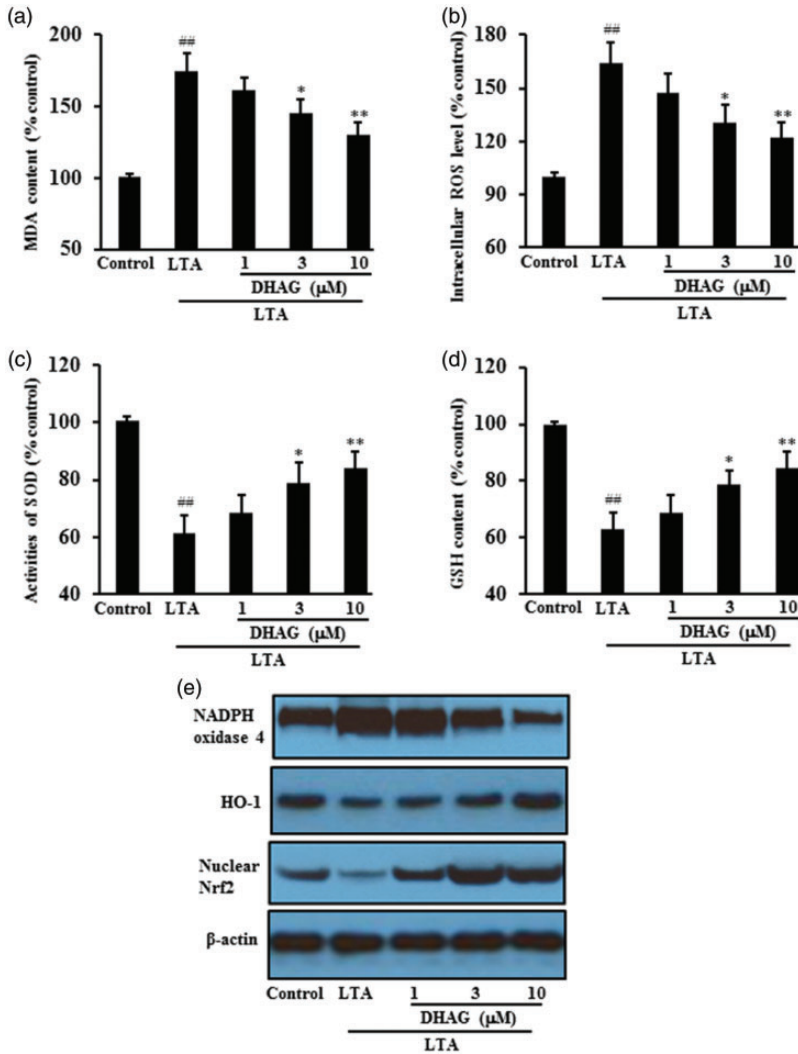
Figure 3. DHAG inhibited oxidative stress in H9c2 cells induced by LTA. H9c2 cells were treated with DHAG at 1, 3, or 10 μM for 6 hours and then treated with LTA for 24 hours. Cells were collected to measure oxidative stress via MDA content (a), intracellular ROS levels (b), SOD activity (c), GSH levels (d) and oxidative stress-related protein expression levels (e). $^{\#\#}p < 0.01$ vs. negative control; $^{*}p < 0.05$, $^{**}p < 0.01$ vs. LTA alone.

involved in inflammatory responses. Cardiomyocytes produce pro-inflammatory cytokines and chronic inflammatory responses can cause oxidative stress, resulting in IE.[17–19] Our results revealed that DHAG attenuated the toxicity of a bacterial component and had anti-inflammatory effects that stimulated cardiomyocytes.

Mitochondria play a pivotal role in the regulation of cell death. Decreased MMP causes mitochondrial fragmentation, generating excessive amounts of ROS and causing
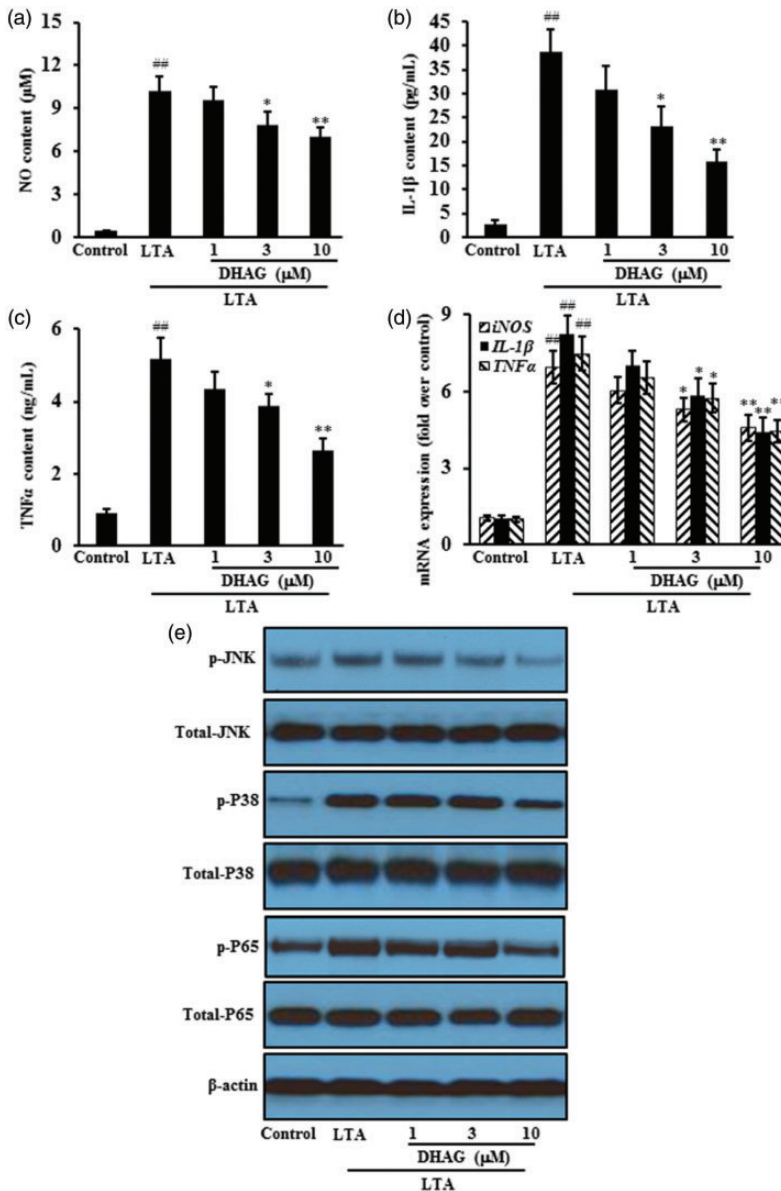
Figure 4. DHAG inhibited inflammatory responses in H9c2 cells induced by LTA. H9c2 cells were treated with DHAG at 1, 3, or 10 μM for 6 hours and then treated with LTA for 24 hours. Inflammatory responses were assessed via NO levels (a); IL-1β levels (b); TNF-α levels (c); mRNA expression (d) and protein expression (e). [##]$p < 0.01$ vs. negative control; *$p < 0.05$, **$p < 0.01$ vs. LTA alone.

damage to mitochondrial structure and function. Eventually, the cellular ATP supply is interrupted and apoptosis is activated.[20,21] Mitochondria modulate cell

viability through ROS-mediated cell oxidative injury and HtrA2/Omi liberation-induced caspase activation.[22,23] As apoptosis effectors, caspase-3 and caspase-9 precursor

activate endonucleases to cleave nuclear DNA, leading to cell death.[24] In this study, LTA treatment caused cell damage as shown by MMP decrease, cytochrome c release, and increased caspase-3 and -9 activities. Anti-apoptotic protein expression decreased, but pro-apoptotic protein expression increased. However, the above effects were largely reversed by DHAG treatment.

Excessive accumulation of ROS can result in oxidative stress. High oxidative stress can induce different cell death programs, including apoptosis, autophagy and necrosis,[25–28] and has been considered as a major cause of cellular injuries in many disorders.[29–31] MDA is well known as a widely-used marker for oxidative damage and resulting thiobarbituric acid reactive substances, whose levels are proportional to the degree of lipid peroxidation and oxidative stress.[32] Therefore, it seems reasonable to use exogenous antioxidants as potential therapeutics to reverse the imbalance between the intracellular oxidative and anti-oxidative systems. The transcription factor Nrf2 is a master regulator of antioxidant and detoxification genes with cytoprotective function.[33] Since Nrf2 inactivation is necessary for the complete execution of apoptosis in the presence of cellular damage caused by oxidative stress, constitutive activation of Nrf2 may protect cells from apoptosis via binding to antioxidant response elements and inducing the expression cytoprotective target proteins such as antioxidant proteins, phase II detoxifying enzymes, and molecular proteasome/chaperones.[34,35] In the present study, DHAG-induced Nrf2 activation was observed. This further induced expression of antioxidant genes to restore oxidative homeostasis, as shown by decreased protein expression of NADPH oxidase 4,a major enzyme responsible for production of superoxide by transferring electrons across the membrane from NAD(P)H to molecular oxygen,[36] reduced levels of MDA and ROS, increased SOD activity and increased GSH levels.

Production of inflammatory cytokines is part of the immune response to many inflammatory stimuli and is involved in the progression of inflammatory diseases.[37,38] DHAG exerted anti-inflammatory effects by inhibiting inflammatory factors including the pro-inflammatory mediator NO and the pro-inflammatory cytokines IL-1β and TNF-α in LTA-stimulated H9c2 cells. Moreover, DHAG considerably suppressed pro-inflammatory molecule production from upstream signaling pathways, which were involved in the progression of inflammatory responses in H9c2 cells. Activation of NF-κB and MAPK leads to transcription factor binding to the promoter regions of pro-inflammatory cytokine genes, thereby enabling transduction of extracellular signals into cellular reactions.[39] DHAG decreased phosphorylation of several MAPKs, including JNK and P38, whose phosphorylation was induced by LTA stimulation. In addition, DHAG reduced nuclear translocation of NF-κB in response to LTA.

Our study demonstrated that DHAG, isolated from the endophytic fungus *P. citrinum* of *B. gymnorrhiza.*, inhibited LTA-induced oxidative stress and inflammatory responses in cardiomyoblasts. Our results provide a scientific rationale for developing DHAG as a therapeutic agent infective endocarditis.

Consent

Patient consent was not applicable as animal and human subjects were not involved in this study.

Declaration of conflicting interest

Ethical approval

Funding

ORCID iD

Xinming Xie   https://orcid.org/0000-0002-8130-8618

References

1. Gupta S, Sakhuja A, McGrath E, et al. Trends, microbiology, and outcomes of infective endocarditis in children during 2000-2010 in the United States. *Congenit Heart Dis* 2017; 12: 196–201.

2. Lockhart PB, Brenman MT, Thornhill M, et al. Poor oral hygiene as a risk factor for infective endocarditis-related bacteremia. *J Am Dent Assoc* 2009; 140: 1238–1244.

3. Zhu L, Zhang Y, Fan J, et al. Characterization of competence and biofilm development of a Streptococcus sanguinis endocarditis isolate. *Mol Oral Microbiol* 2011; 26: 117–126.

4. Rodriguez AM, Callahan JE, Fawcett P, et al. Physiological and molecular characterization of genetic competence in Streptococcus sanguinis. *Mol Oral Microbiol* 2011; 26: 99–116.

5. Sanchez-Rodriguez F, Rivera R, Suarez-Gonzalez J, et al. Prevention of infective endocarditis: a review of the American Heart Association guidelines. *Bio Asoc Med P R* 2008; 100: 25–28.

6. Farbod F, Kanaan H and Farbod J. Infective endocarditis and antibiotic prophylaxis prior to dental/oral procedures: latest revision to the guidelines by the American Heart Association published April 2007. *Int J Oral Maxillofac Surg* 2009; 38: 626–631.

7. Moss DW and Bates TE. Activation of murine microglial cell lines by lipopolysaccharide and interferon-gamma causes NOmediated decreases in mitochondrial and cellular function. *Eur J Neurosci* 2001; 13: 529–538.

8. Kochan T, Singla A, Tosi J, et al. Toll-like receptor 2 ligand pretreatment attenuates retinal microglial inflammatory response but enhances phagocytic activity toward *Staphylococcus aureus*. *Infect Immun* 2012; 80: 2076–2088.

9. Gutierrez-Venegas G, Alonso LO, Ventura-Arroyo JA, et al. Myricetin suppresses lipoteichoic acid induced interleukin-1β and cyclooxygenase-2 expression in human gingival fibroblasts. *Microbiol Immunol* 2013; 57: 849–856.

10. Onyango IG and Khan SM. Oxidative stress, mitochondrial dysfunction, and stress signaling in Alzheimer's disease. *Curr Alzheimer Res* 2006; 3: 339–349.

11. Ostrowski S, Kasielski M, Kordiak J, et al. Myocardial oxidative stress in patients with active infective endocarditis. *Int J Cardiol* 2013; 167: 270–276.

12. Kang K and Yu MZ. Protective effect of sulforaphane against retinal degeneration in the $Pde6^{rd10}$ mouse model of retinitis pigmentosa. *Curr Eye Res* 2017; 42: 1684–1688.

13. Hu SL and Zheng CP. (3R)-5,6,7-trihydroxy-3-isopropyl-3-methylisochroman-1-one ameliorates retinal degeneration in Pde6b^{rd10} mice. *Cutan Ocul Toxicol* 2018; 37: 245–251.

14. Jin W, Xu X, Chen X, et al. Protective effect of pig brain polypeptides against corticosterone-induced oxidative stress, inflammatory response, and apoptosis in PC12 cells. *Biomed Pharmacother* 2019; 115: 108890. DOI: 10.1016/j.biopha.2019.108890.

15. Wu YZ, Qiao F, Xu GW, et al. Neuroprotective metabolites from the endophytic fungus *Penicillium citrinum* of the mangrove *Bruguiera gymnorrhiza*. *Phytochem Lett* 2015; 12: 148–152.

16. Schmölz L, Wallert M and Lorkowski S. Optimized incubation regime for nitric oxide measurements in murine macrophages

using the Griess assay. *J Immunol Methods* 2017; 449: 68–70.

17. Palomer X, Salvado L, Barroso E, et al. An overview of the crosstalk between inflammatory processes and metabolic dysregulation during diabetic cardiomyopathy. *Int J Cardiol* 2013; 168: 3160–3172.

18. Cognasse F, Hamzeh-Cognasse H, Chabert A, et al. *Streptococcus sanguinis* induced cytokine and matrix metalloproteinase-1 release from platelets. *BMC Immunol* 2014; 15: 15–20.

19. Watkin RW, Harper LV, Vernallis AB, et al. Pro-inflammatory cytokines IL6, TNF-alpha, IL1beta, procalcitonin, lipopolysaccharide binding protein and C-reactive protein in infective endocarditis. *J Infect* 2007; 55: 220–225.

20. Wang H, Zhao X, Ni C, et al. Zearalenone regulates endometrial stromal cell apoptosis and migration via the promotion of mitochondrial fission by activation of the JNK/Drp1 pathway. *Mol Med Rep* 2018; 17: 7797–7806.

21. Geng C, Wei J and Wu C. Yap-Hippo pathway regulates cerebral hypoxia-reoxygenation injury in neuroblastoma N2a cells via inhibiting ROCK1/F-actin/mitochondrial fission pathways. *Acta Neurol Belg* 2018; in press. doi: 10.1007/s13760-018-0944-6.

22. Li H, He F and Zhao X. YAP inhibits the apoptosis and migration of human rectal cancer cells via suppression of JNK-Drp1-mitochondrial fission-HtrA2/Omi pathways. *Cell Physiol Biochem* 2017; 44: 2073–2089.

23. Lei Q, Tan J, Yi S, et al. Mitochonic acid 5 activates the MAPK-ERK-yap signaling pathways to protect mouse microglial BV-2 cells against TNFalpha-induced apoptosis via increased Bnip3-related mitophagy. *Cell Mol Biol Lett* 2018; 23: 14.

24. Xin BR, Liu JF, Kang J, et al. (2R, 3S)-pinobanksin-3-cinnamate, a new flavonone from seeds of Alpinia galanga willd., presents in vitro neuroprotective effects. *Mol Cell Toxicol* 2014; 10: 165–172.

25. Felton GW and Summers CB. Antioxidant systems in insects. *Arch Insect Biochem Physiol* 1995; 29: 187–197.

26. Radogna F, Cerella C, Gaigneaux A, et al. Cell type-dependent ROS and mitophagy response leads to apoptosis or necroptosis in neuroblastoma. *Oncogene* 2016; 35: 3839–3853.

27. Vaseva AV, Marchenko ND, Ji K, et al. p53 opens the mitochondrial permeability transition pore to trigger necrosis. *Cell* 2012; 149: 1536–1548.

28. Luckhart S, Giulivi C, Drexler AL, et al. Sustained activation of Akt elicits mitochondrial dysfunction to block Plasmodium falciparum infection in the mosquito host. *PLoS Pathog* 2013; 9: e1003180.

29. Halliwell B. Oxidative stress and neurodegeneration: where are we now? *J Neurochem* 2006; 97: 1634–1658.

30. Uguz AC and Naziroglu M. Effects of selenium on calcium signaling and apoptosis in rat dorsal root ganglion neurons induced by oxidative stress. *Neurochem Res* 2012; 37: 1631–1638.

31. Birben E, Sahiner UM, Sackesen C, et al. Oxidative stress and antioxidant defense. *World Allergy Organ J* 2012; 5: 9–19.

32. Xiao X, Liu J, Hu J, et al. Protective effects of protopine on hydrogen peroxide-induced oxidative injury of PC 12 cells via Ca2+ antagonism and antioxidant mechanisms. *Eur J Pharmacol* 2008; 591: 21–27.

33. Mendez-Garcia LA, Martinez-Castillo M, Villegas-Sepulveda N, et al. Curcumin induces p53-independent inactivation of Nrf2 during oxidative stress-induced apoptosis. *Hum Exp Toxicol* 2019; 38: 951–961. doi: 10.1177/0960327119845035.

34. Kobayashi M and Yamamoto M. Nrf2-Keap1 regulation of cellular defense mechanisms against electrophiles and reactive oxygen species. *Adv Enzyme Regul* 2006; 46: 113–140.

35. Jaiswal AK. Regulation of antioxidant response element-dependent induction of detoxifying enzyme synthesis. *Methods Enzymol* 2004; 378: 221–238.

36. Bedard K and Krause KH. The NOX family of ROS-generating NADPH oxidases: physiology and pathophysiology. *Physiol Rev* 2007; 87: 245–313.

37. Yu MZ, Kang K, Bu P, et al., Deficiency of CC chemokine ligand 2 and decay-accelerating factor causes retinal

degeneration in mice. *Exp Eye Res* 2015; 138: 126–133.

38. Cho W, Nam JW, Kang HJ, et al. Flower extract of Panax notoginseng attenuates lipopolysaccharide-induced inflammatory response via blocking of NF-κB signaling pathway in murine macrophages. *Int Immunopharmacol* 2009; 9: 1049–1057.

39. Dong C, Davis RJ and Flavell RA. MAP Kinases in the immune response. *Annu Rev Immunol* 2002; 20: 55–72.